Pulsed Field Separation of Biomolecules

in a Nanofluidic Filter Array

by

Noel I. Reyes González

Submitted to the Department of Electrical Engineering and Computer Science

in Partial Fulfillment of the Requirements for the Degrees of

Bachelor of Science in Electrical [Computer] Science and Engineering

and Master of Engineering in Electrical Engineering and Computer Science

at the Massachusetts Institute of Technology

February 3, 2006

Author_____
Department of Electrical Engineering and Computer Science
February 3, 2006

Certified by_____
Jongyoon Han
Thesis Supervisor

Accepted by_____
Arthur C. Smith
Chairman, Department Committee on Graduate Theses

Pulsed Field Separation of Biomolecules in a Nanofluidic Filter Array
by
Noel I. Reyes González

Submitted to the
Department of Electrical Engineering and Computer Science

February 3, 2006

In Partial Fulfillment of the Requirements for the Degree of
Bachelor of Science in Electrical [Computer] Science and Engineering
and Master of Engineering in Electrical Engineering and Computer Science

ABSTRACT

In this work, pulsed electric fields are introduced as a means to enhance separation efficiency of biomolecules in a nanofluidic filter array channel. Separation under pulsed fields was tested using PBR322 DNA, Lambda Hind III DNA, and a sample containing three SDS denatured proteins. Pulsed fields are divided into long pulse and short pulse regimes, depending on how long the duration of the higher electric field pulse is compared to the average trapping time of a molecule in a single nanofluidic filter. It was found that under long pulse fields, the separation selectivity cannot be enhanced since the difference in velocity between two different molecules will always be a weighted average of the velocity at the high and low field levels of the pulsed field. On the other hand, application of pulsed fields in the short pulse regime yielded more promising results. After the pulse duration became comparable to the average trapping time of migrating molecules, the average velocity of molecules decreased with a reduction in the pulse duration. Certain bands within a sample were slowed down more than others by appropriately choosing the pulse duration, therefore resulting in increased selectivity and higher separation efficiency. For PBR322 DNA, separation resolution of up to 2.54 was obtained in under 15 minutes when the pulse duration was decreased down to 5ms. Novel experiments are proposed to achieve separation through band selective elution and bidirectional transport. A probabilistic model based on the binomial distribution is also proposed as a method to estimate the average velocity of molecules in the short pulse regime.

Thesis Supervisor: Jongyoon Han
Title: Karl Van Tassel Assistant Professor of Electrical Engineering, Department of Electrical Engineering and Computer Science and Assistant Professor of Biological Engineering, Biological Engineering Division.

Table of Contents

1. Introduction

The use of microfluidic and nanofluidic devices has proven useful in many areas, including the analysis of complex biological samples [1, 2]. Improvements in the field of microfabrication have made it possible to reduce the feature size of these devices to 1~100 nanometers, which is comparable to the size of biological molecules like proteins and DNA. Recently, a nanofluidic filter device with the capability of sorting biological molecules by size was developed by Han et al [3]. As illustrated in Fig. 1, the device consists of a series of intercalated thin and deep channels through which the biomolecules flow suspended in a saline buffer. The biomolecules, having a net negative charge, are driven down the length of the nanofluidic filter channel by applying an electric field across the two ends of the channel. The "deep to thin" channel transition acts as a trap to the biomolecules that pass by. The level of trapping at each one of these transitions is dependent on the size of the biomolecule. Depending on the trapping mechanism in effect, some biomolecules will escape the trap faster than others, therefore molecules of different size have a different average mobility as they migrate across the length of the nanofluidic filter channel.

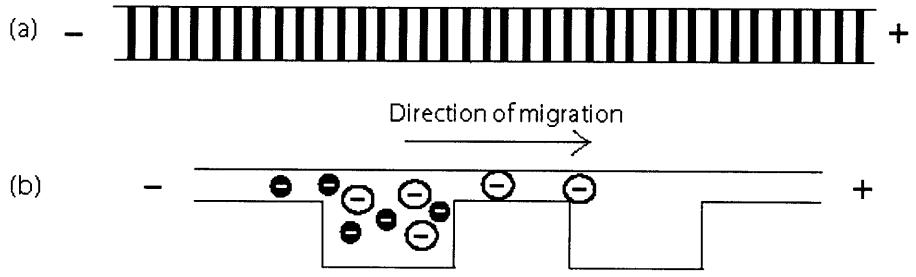

Figure 1. (a) Series of intercalated thin and deep nanofilters through the length of the channel. **(b)** Negatively charged molecules move through the channel, being driven by the applied electric field. One group of molecules moves faster than the second group of molecules.

The time that it takes for a molecule to escape one single trap in described by some probability density function depending on the trapping mechanism in effect. It has been proposed that when the size of a biomolecule is large compared to the thin region of the nanofluidic filter, the biomolecule is trapped by entropic trapping [3]. The mechanism gets its name from the fact that a molecule is trapped because it is favored by the entropic free energy in the deep regions of the channel. It was determined that DNA molecules of larger size escape the traps faster, as having more monomers facing the entrance of the thin region makes it easier to overcome the free energy difference between the two regions. On the contrary, when the biomolecule is relatively smaller than the thickness of the thin channel, the molecules are effectively trapped by Ogston sieving [4]. In this case, steric repulsion does not allow certain angular conformations of a molecule near a channel wall, therefore making it more favorable for molecules of smaller size to move through a thin channel region faster. For either trapping mechanism in effect, an average trapping time can be estimated as a function of molecule size, electric field intensity, and nanofluidic filter dimensions [3, 4].

Pulsed-field gel electrophoresis was implemented about twenty years ago for the separation of large DNA molecules [5]. Pulsed fields and other types of alternating field have been since used to improve already existing separation techniques [6], while they have never been used for the type of nanofluidic channels mentioned above. Just as in gel electrophoresis, it is believed that alternating fields might provide the chance for enhanced separation by directly affecting the dynamics and mechanics of biomolecules migrating across a set of nanofluidic filters.

Computer simulations that solve the migration of polyelectrolytes in a nanofluidic channel like the one used in our experiments, were carried out and reported by Slater et al in [7]. Their study is motivated based on the fact that the dependence of mobility on the applied electric field in highly non-linear, and the implications of utilizing complex types of electric fields as the driving force may not be easily characterized analytically. The authors found that applying different types of pulsed electric fields, the order of band elution can be altered. An extension to the analysis of this idea shows that it is also possible to make different bands within a sample to move in opposite directions [8]. Varying the frequency of the applied pulsed field, presents the possible existence of a resonant frequency at which the velocity of the molecules is maximized without considerably affecting the separation efficiency. Finally, when applying a high frequency square field, the average mobility of a molecule appears to converge to the average of the two field levels in the pulsed field.

Separation of large DNA, small DNA, and proteins has been now achieved with the use of this type of nanofluidic filter channels. Recently, separation of small DNA and proteins was achieved in less than 10 minutes. The focus of this paper is to discuss the possibility of utilizing pulsed fields to enhance the efficiency of separation. Chapter 2 introduces the theory behind the use of pulsed fields, and describes the difference between the long and short pulse regimes. The experimental results are discussed in Chapter 5 together with additional theory introduced to support the obtained results.

2. Theory

In pulsed field separation of biomolecules, a square wave field like that in Fig. 2 is applied to drive the flow of molecules along the set of nanofluidic filters. There are

four parameters that entirely describe the form of this field. The first two parameters are the high and low electric field values, which are denoted as $\mathbf{E_H}$ and $\mathbf{E_L}$ respectively in Fig. 2. The other two parameters represent the duration of the pulse at each field level, t_H being the pulse duration at the field level $\mathbf{E_H}$, and t_L being the pulse duration at the field level $\mathbf{E_L}$.

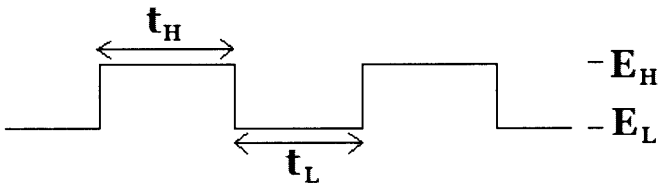

Figure 2. Example of square wave field used in pulsed field separation. $\mathbf{E_H}$ and $\mathbf{E_L}$ are the high and low electric fields levels of the pulsed field. Parameters t_H and t_L are the pulse durations at the high and low electric fields respectively.

2.1 - Pulsed Field Separation: Long Pulse Regime

Long pulses are defined as those with a duration that is large compared to the average trapping time of the molecule at the low electric field level $\mathbf{E_L}$. It is expected that for field durations, t_H and t_L, that are considerably larger than the average trapping time, the dynamics of the trapping effect caused by the nanofluidic filters will not be altered. If the trapping dynamics are not altered by applying the pulsed field, the average velocity of a molecule should be the average of the velocities at field levels $\mathbf{E_H}$ and $\mathbf{E_L}$. The latter statement is described by the following equation:

$$v_{AV} = \frac{\mu_H E_H t_H + \mu_L E_L t_L}{t_H + t_L} = \frac{\mu_H E_H \frac{t_H}{t_L} + \mu_L E_L}{1 + \frac{t_H}{t_L}}. \qquad (1)$$

For the special case where $\mathbf{t_H} = \mathbf{t_L}$, we have that:

$$v_{AV} = \frac{\mu_H E_H + \mu_L E_L}{2}. \qquad (2)$$

By inspection of (1) and (2) it follows that the absolute values of t_H and t_L do not determine the value of the average velocity in the long pulse regime. The speed of the molecules is rather dependent on the ratio of the two pulse durations. Because the amount of separation between molecules of different size is mainly determined by the difference in average velocities, separation efficiency is not expected to change for different long pulses as long as the ratio between the two pulse durations is kept constant.

2.2 - Pulsed Field Separation: Short Pulse Regime

The short pulse regime consists of those pulsed field signals for which the pulse durations, t_H and t_L, are equal to or smaller than the average trapping time of any band in the sample being separated. If the average trapping times of the different bands in a sample are known for a certain electric field level, short pulse duration fields might enhance separation between bands. For the sake of simplicity, a sample with only two bands is considered in the description of the model. If the field level is maintained for an amount of time longer than the average trapping time of the fastest molecule, but shorter than the average trapping time of the slowest molecule, it is possible to provoke elution of the first molecule from the trap while leaving the slower molecule behind.

Fig. 3 shows an example of enhanced separation under the short pulse regime, considering that trapping occurs through the Ogston sieving mechanism so that smaller molecules elude the traps faster than the larger molecules. The illustration shows two groups of different size molecules floating around the deep region of the channel (A). An electric field is suddenly stepped from E_L to E_H and maintained at E_H for a time greater than the average trapping time of the smaller molecule and lower than the average

trapping time of the bigger molecule. Smaller molecules sense the field for long enough time so that they can elude the trap (B). Some of the bigger molecules might also get to elude the trap but most of them will stay behind in the first deep region. Finally, the field is turned back to level E_L and remains at that value for a time smaller than the average trapping time of both bands. Molecules in the thin region of the channel are allowed to move to the next deep region, and those that previously did not escape the trap remain still in the first deep region (C).

The average trapping time mentioned in step B is that of the molecules at electric field level E_H, while the average trapping time mentioned in step C is that of the molecules at electric field level E_L.

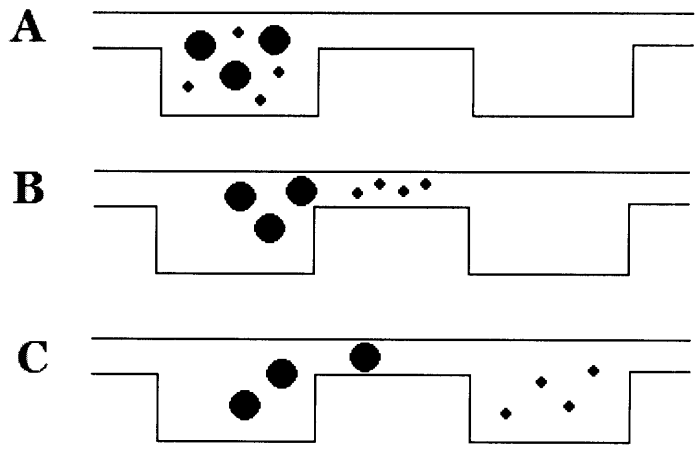

Figure 3. Selective elution of a single trap by choosing the duration of the short pulse field to be between the average trapping times of both molecules in the sample. **A.** Both groups of molecules float around the deep region of the channel. **B.** The electric field is suddenly stepped from E_L to E_H and maintained at E_H for a time greater than the average trapping time of the smaller molecule and lower than the average trapping time of the bigger molecule. Smaller molecules sense the field for long enough time so that they can elude the trap. Some of the bigger molecules might also get to elude the trap but most of them will stay behind in the first deep region. **C.** The field is turned back to level E_L and remains at that value for a time smaller than the average trapping time of both bands. Molecules in the thin region of the channel are allowed to move to the next deep region, and those that previously did not escape the trap remain still in the first deep region.

Continuously switching from field level E_H to E_L and back would repeat these three steps, every time inducing movement along the channel of the smaller molecules, while holding the majority of the larger molecules from being able to escape the traps. In this way, a pulsed field in the short pulse regime could enhance separation of two different bands in a sample.

3. Methods

3.1 – Experimental Setup and Procedure

The nanofilter channels were etched in a silicon wafer, and holes were etched through the whole thickness of the silicon where reservoirs were to be installed. The wafer was then bonded to glass on the etched side and plastic reservoirs were glued with silicone rubber where the holes were made. The reservoirs were filled up with 5x Tris-Borate-EDTA (TBE) buffer. To ensure the whole length of the nanofilter channel was filled with the TBE buffer, electroosmotic flow was induced by applying an electric field across the two ends. Two types of DNA samples were used for the separation experiments. PBR322 and Lambda Hind III from New England Biolabs were labeled with YOYO-1 dye at a concentration of 1μM. DTT at a concentration of 0.1mM was added to prevent degradation of the fluorescence intensity. Protein experiments,were also performed with the samples mentioned in section 4.2. Additional 0.1wt% sodium dodecyl sulfate (SDS, Sigma) was added to denature the proteins, and were then conjugated with fluorescein or Alexa Fluor 488 (Molecular Probes). The final mixture was incubated in a 65°C water bath for 10 minutes.

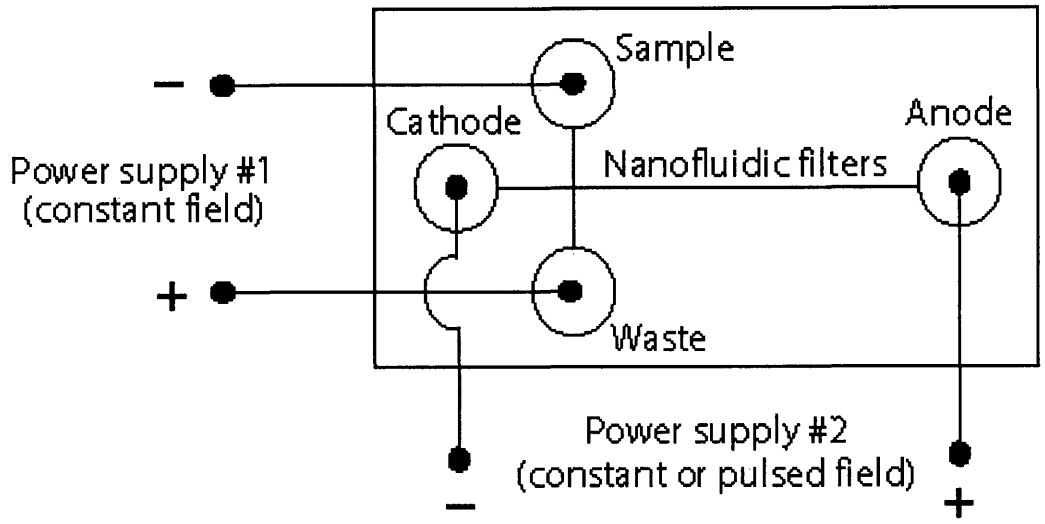

Figure 4. Schematic of device setup. Two separate power supplies with their ground nodes connected were used to apply electric fields across the ends of the channel.

Platinum wires inserted inside the reservoirs were used as electrodes. Standard wire connections were made between the electrodes and two power supplies. The first power supply, a PS325/2500V from Stanford Research Systems, was used to apply a constant voltage across the sample and waste reservoirs as shown in Fig. 4. A second power supply, a LabSmith HVS448 High Voltage Sequencer, was used to apply either a constant or a pulsed voltage across the nanofilter channel. The ground nodes of both power supplies were connected together to establish a common ground. A serial cable connected the power supply to a personal computer. LabSmith Sequencer software was utilized to control the intensity and pulse duration of the applied field. An Olympus IX71 inverted microscope was used to observe the fluorescence of the molecules through the glass side of the device. The image observed through the microscope was viewed and recorded with the use of a Cooke Sensicam CCD camera and IPLab Imaging Software.

3.2 - Analysis of extracted data

After the data was collected from the series of experiments, the fluorescence intensity of the sample under observation was plotted versus migration time. A Gaussian curve was fitted to each peak in the fluorescence intensity profile, and the mean and standard deviation were measured for each peak. Separation efficiency was characterized by measuring the resolution R between adjacent peaks, which is given by

$$R = \frac{\Delta t}{\Delta t_1 + \Delta t_2}. \tag{3}$$

In (3), Δt stands for the difference in time between the mean values of two adjacent peaks, m_1 and m_2. The quantities Δt_1 and Δt_2 are two times the standard deviations, σ_1 and σ_2, for each one of the two peaks. Fig. 5 is an example of the measurements made to calculate the separation resolution. With this definition for the resolution, a value of $R > 1$ means that the peaks were separated with baseline resolution.

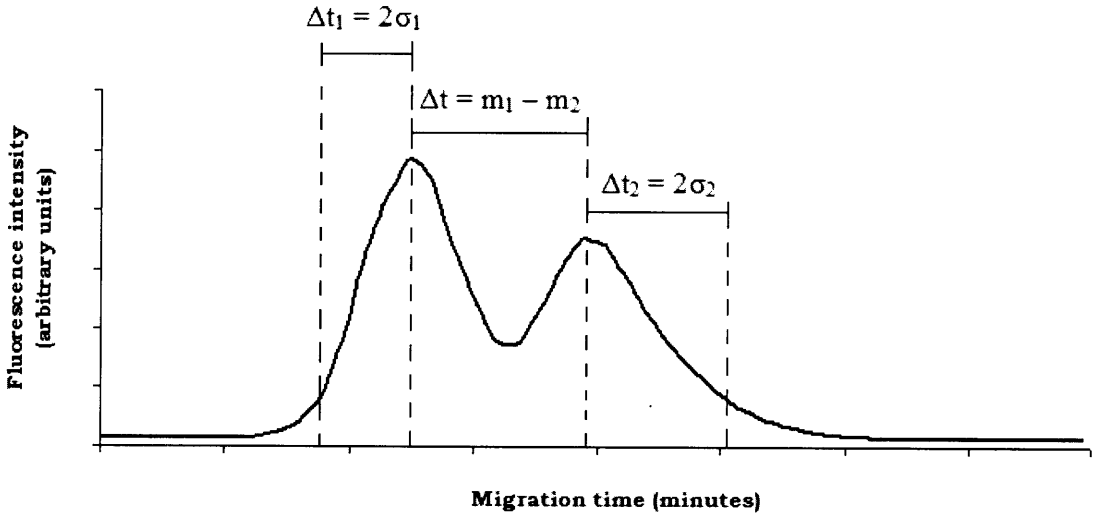

Figure 5. Example of measurements made to calculate the separation resolution.

Experimental average trapping times were also calculated to understand the results obtained from pulsed field experiments. The average trapping time τ_{ave} can be determined experimentally by solving for it in the following equation:

$$\frac{\mu}{\mu_{\max}} = \frac{t_{travel}}{t_{travel} + \tau_{ave}}, \tag{4}$$

where μ is the measured average mobility of a band of molecules driven at a certain electric field intensity, $\mu_{\max}$ is the maximum mobility that is possibly attainable within the nanofilter channel, and t_{travel} is the time it takes to travel one thin plus one deep region.

4. Results

4.1 – Large DNA: Entropic Trapping Regime

Lambda Hind III DNA has bands of 23, 9, 6, and 4 kilobasepairs. The radius of gyration of these molecules is considerably larger than 60 nm, the thickness of the thin region in the device used for this set of experiments. Results of separation in constant field separation experiments are presented first, followed by the results obtained when using long pulse fields.

4.1.1 – Constant Field Separation Results

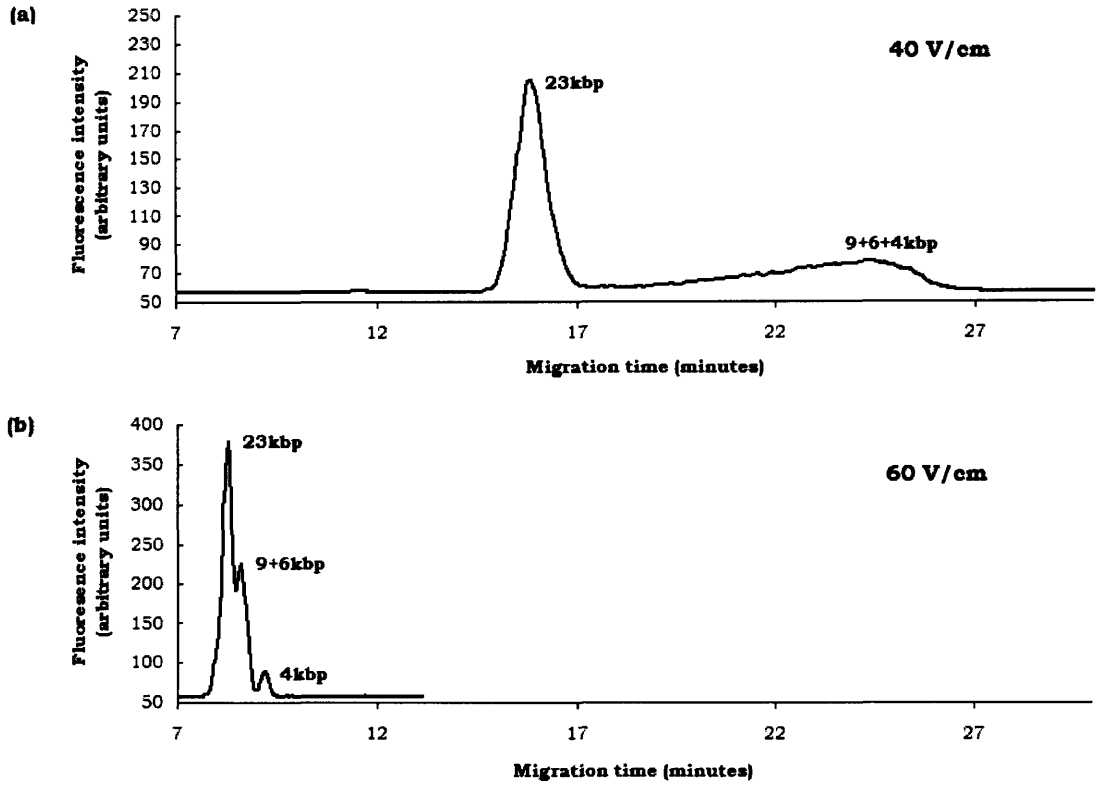

Figure 6. Fluorescence intensity for constant field separation of Lambda Hind III DNA.

Standard, constant field separation trials were carried out to determine the separation efficiency and make estimates of the average trapping time of Lambda Hind III molecules at different electric field levels. Separation results for electric fields of 40 and 60 V/cm are shown in Fig. 6. Fluorescence intensity was measured 1 cm down the nanofilter channel for both cases. At 40 V/cm two peaks are observed. The peaks for the three smallest bands in the sample are not distinguishable, but the 23 kb band is efficiently separated from the rest. Running separation at 60 V/cm shows an additional peak, but the resolution is largely affected. Separation resolution values for both

experiments are shown in Table 1, while the average mobility and average trapping time values obtained experimentally are shown in Table 2.

Table 1. Separation resolution between adjacent peaks Lambda Hind III for a constant field separation experiment.

Bands	*R* (40 V/cm)	*R* (60 V/cm)
23 & 9 kbp	2.85	0.47
9 & 6 kbp	0	0
6 & 4 kbp	0	1.2

Table 2. Average mobility and average trapping time for bands of Lambda Hind III. *This is the average trapping time estimated using equation (4), but the real average trapping time must in reality be a positive number very close to zero.

Band size (kbp)	μ at 40 V/cm (cm^2/V·min)	μ at 60 V/cm (cm^2/V·min)	τ_{ave} at 40 V/cm (ms)	τ_{ave} at 60 V/cm (ms)
23	0.0017	0.0021	100	0*
9	0.0011	0.0020	392	10
6	0.0011	0.0020	392	10
4	0.0011	0.0019	392	32

4.1.2 – Pulsed Field Separation Results: Long Pulse Regime

Pulsed field separation trials in the long pulse regime were also carried out utilizing the Lambda Hind III sample. The applied pulsed field stepped from $\mathbf{E_H}$ = 60 V/cm to $\mathbf{E_L}$ = 40 V/cm with pulse durations of $t_H = t_L = 3$ seconds for the first trial and $t_H = t_L = 1$ second for the second trial. Fluorescence intensity profiles for both cases are essentially identical (see Fig. 7). Baseline resolution was not obtained between any of the bands in the sample, but the 23 kb molecules are partially separated from the other bands. Values for the separation resolution are shown in Table 3.

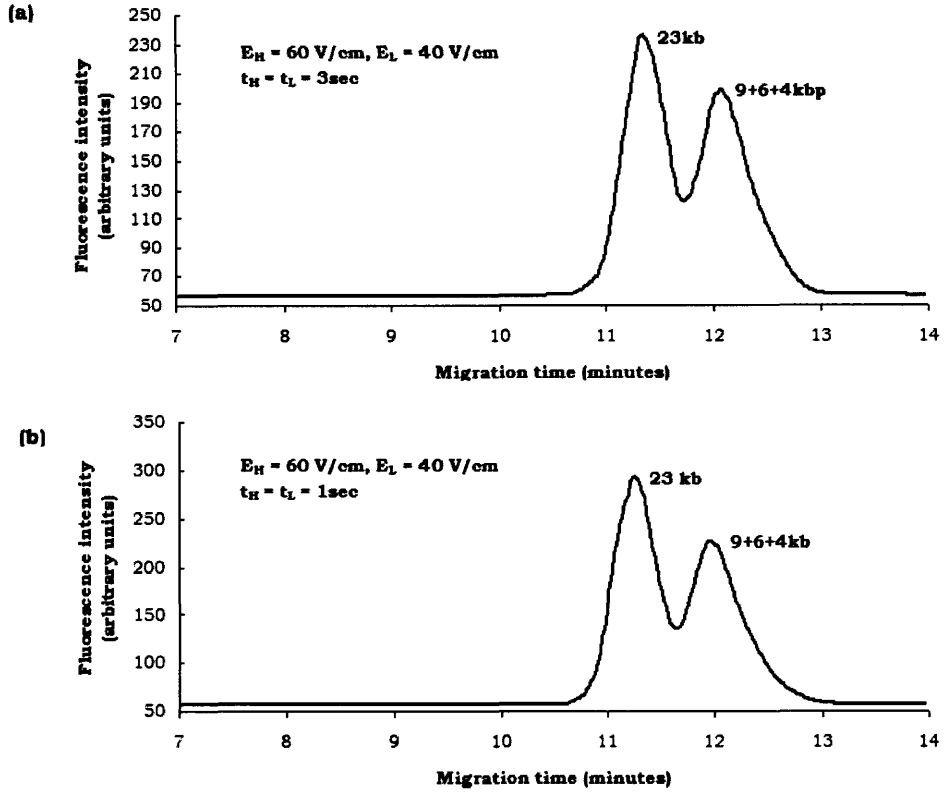

Figure 7. Fluorescence intensity for long pulse field separation of Lambda Hind III DNA.

Table 3. Separation resolution between adjacent peaks Lambda Hind III for a long pulse regime separation experiment.

Bands	R (t_H=t_L=3sec)	R (t_H=t_L=1sec)
23 & 9 kbp	0.63	0.65
9 & 6 kbp	0	0
6 & 4 kbp	0	0

4.2 – SDS Proteins: Ogston Sieving Regime

The SDS protein sample was composed of cholera toxin subunit B (CT-B), lectin phytohemagglutinin-L (PHA-L), and low density human lipoprotein (LDL). The molecular weights of the three types of protein are 11.4kDa, 120kDa, and 179kDa respectively. Separation results are shown for the both constant and pulsed field experiments. The nanofilter channel had thin and deep regions of 60 and 250 nm respectively. Fluorescence intensity measurements were made at a distance of 0.25 cm along the nanofilter channel for

all experiments. It is known that these proteins are smaller than 50nm, so that the difference in mobility between molecules results as an effect of Ogston sieving in the thin region of the nanofluidic filter channel [4].

4.2.1 – Constant Field Separation Results

Fluorescence intensity profiles for constant field separation of SDS proteins are shown in Fig. 8 for electric field levels of 130, 100, 80, and 60 V/cm. PHA-L and LDL only have individual distinguishable peaks in the 80 V/cm case. CT-B is separated from the other bands at every field value, although not with baseline resolution. Numerical values for the resolution between peaks are shown in Table 4. Table 5 shows the average mobility and average trapping time of the three SDS proteins at field intensities of 130 and 60 V/cm.

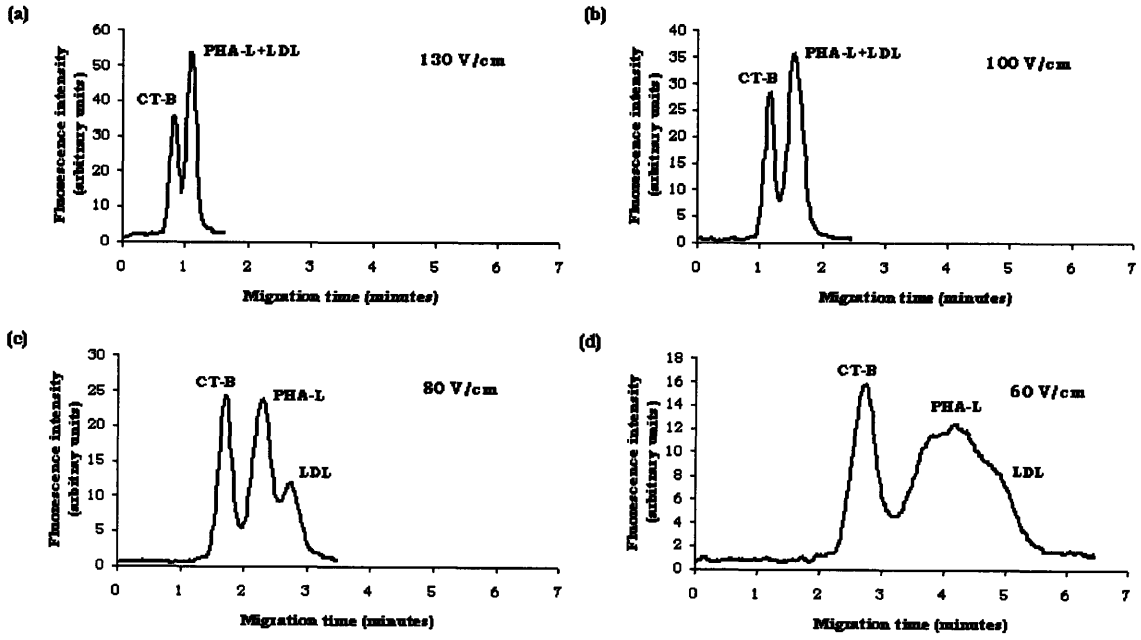

Figure 8. Fluorescence intensity profiles for constant field separation of SDS proteins.

Table 4. Separation resolution between bands of SDS protein sample.

Bands	*R* (130 V/cm)	*R* (100 V/cm)	*R* (80 V/cm)	*R* (60 V/cm)
CB-T& PHA-L	0.77	0.83	0.94	0.80
PHA-L & LDL	0	0	0.68	0.26

Table 5. Average mobility and average trapping time for bands in protein sample. *This is the average trapping time estimated using equation (4), but in reality the average trapping time cannot be zero unless the molecule becomes infinitely small.

Band	μ at 60 V/cm ($cm^2/V \cdot min$)	μ at 130 V/cm ($cm^2/V \cdot min$)	τ_{ave} at 60 V/cm (ms)	τ_{ave} at 130 V/cm (ms)
CB-T	0.0018	0.0025	20	0*
PHA-L	0.0013	0.0019	46	7
LDL	0.0010	0.0019	75	7

4.2.2 – Pulsed Field Separation Results

Pulsed field separations trials were performed for pulse durations between 10 and 500 ms. The results are shown in Figs. 9 & 10 for in order of decreasing pulse duration, and the electrophoregrams for the long pulse regime are separated from those of the short pulse regime. Differentiation between the two regimes was done based on the average trapping times shown in Table 5.

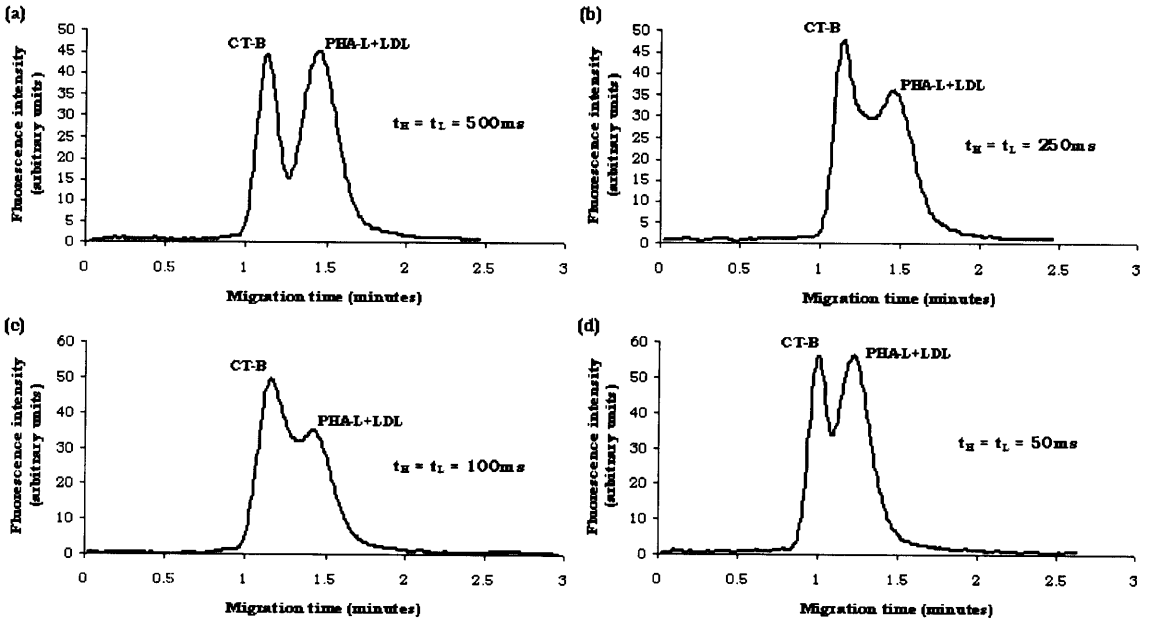

Figure 9. Fluorescence intensity for long pulse field separation of SDS proteins.

By inspection of the electrophoregrams in Fig. 9 it is clear that the migration time is not greatly affected by the change in pulse duration from 500 ms to 50 ms, although the resolution between the two discernible peaks is degraded somewhat as the pulse duration decreases. Table 6 shows how the resolution between the distinguishable bands changed as the pulse duration was varied.

Table 6. Separation resolution between bands of the SDS proteins sample for long pulse regime separation trials.

Bands	R (t_H=t_L=500ms)	R (t_H=t_L=250ms)	R (t_H=t_L=100ms)	R (t_H=t_L=50ms)
CT-B & PHA-L	0.68	0.74	0.55	0.53
PHA-L & LDL	0	0	0	0

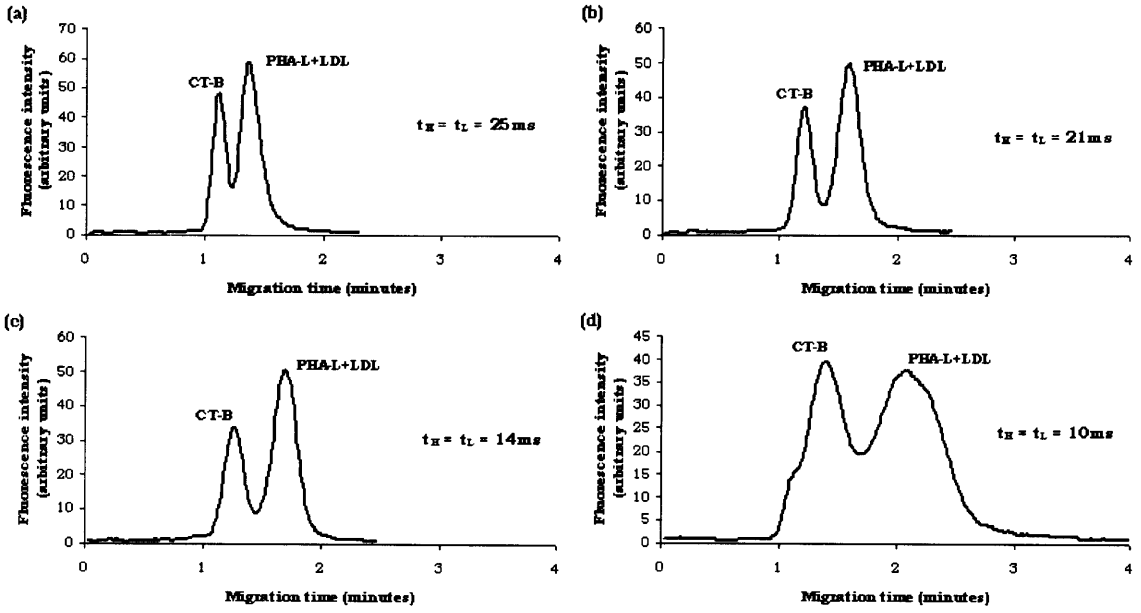

Figure 10. Fluorescence intensity for short pulse field separation of SDS proteins.

For the electrophoregrams in Fig. 10, it is noticeable instead that the average velocity is affected as the peaks shift to the right as the pulse duration decreases. Values for the separation resolution between the distinguishable bands are shown in Table 7 for experiments in the short pulse regime.

Table 7. Separation resolution between bands of the SDS proteins sample for short pulse regime separation trials.

Bands	R (t_H=t_L=25ms)	R (t_H=t_L=21ms)	R (t_H=t_L=14ms)	R (t_H=t_L=10ms)
CT-B & PHA-L	0.74	0.86	0.94	0.64
PHA-L & LDL	0	0	0	0

4.3 – Small DNA: Ogston Sieving Regime

PBR322 DNA was used for the following set of experiments. This sample contains bands of 121, 383, 929, 1058, and 1857 base pairs. The size of these molecules is smaller than the 60nm width of the thin channel region of the channel, and just as the SDS proteins, these DNA molecules experience Ogston sieving as they migrate across the nanofluidic filters.

4.3.1 – Constant Field Separation Results

The electrophoregrams for constant field separation experiments are presented in Fig. 11 for various electric field levels. Fluorescence intensity was measured at a distance of 0.5 cm along the separation column for all experiments. The electrophoregrams show that the separation resolution increases as the electric field decreases from 55 to 25 V/cm. Baseline resolution between peaks 4 and 5 is obtained only when the electric field goes down to 25 V/cm, case at which it takes 53 minutes for the slowest molecules to migrate a distance of 0.5 cm.

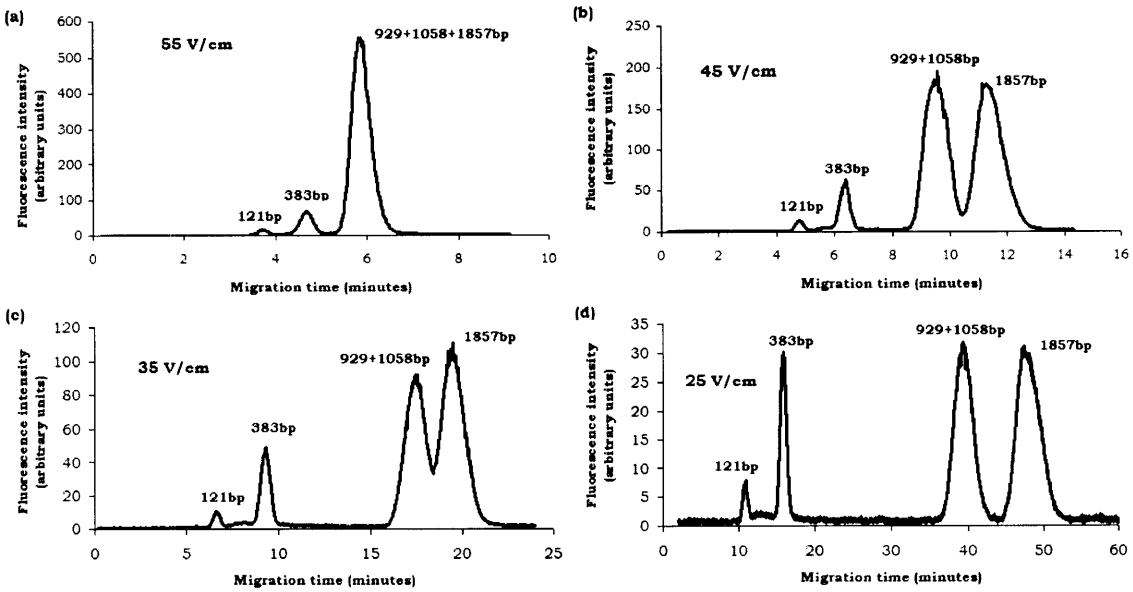

Figure 11. Fluorescence intensity for constant field driven experiments.

Table 8. Separation resolution between adjacent peaks of PBR322 DNA for a constant field separation experiment.

Peaks	*R* (55 V/cm)	*R* (45 V/cm)	*R* (35 V/cm)	*R* (25 V/cm)
121bp & 383bp	1.41	2.29	2.13	2.44
383bp & 929+1058bp	0.76	2.52	3.66	4.84
929+1058bp & 1857bp	0	0.82	0.52	1.27

The graph in Fig. 12 shows the relation between mobility and electric field level for all bands in the PBR322 sample. The average mobility was determined from the average migration time of each band, the position of each peak in the electrophoregrams of Fig. 10. The curves show that in general the average mobility decreases with decreasing electric field. The mobility difference between the various curves increases with decreasing electric field, representative of the enhancement in separation resolution as the electric field decreases. The smoothed curves that cross the data points show the probable trend of the average mobility curves for the range of electric field values between 0 and 70 V/cm.

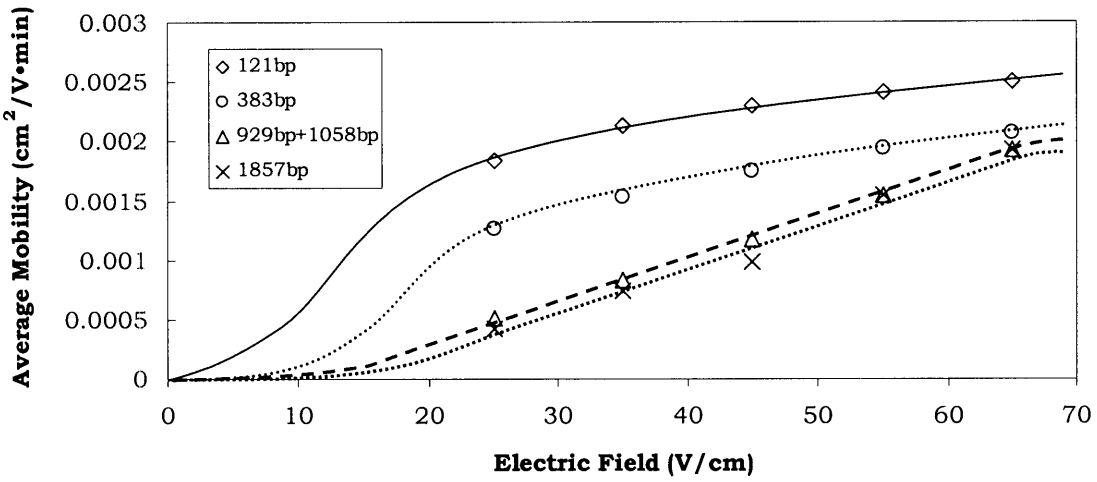

Figure 12. Graph of average mobility versus electric field intensity.

Table 9. Average mobility and average trapping time for bands of PBR322 DNA. *This is the average trapping time estimated using equation (4), but in reality the average trapping time cannot be zero unless the molecule becomes infinitely small. The average trapping time for a 100bp DNA molecule was reported to be ~8ms in [4].

Band size (bp)	μ at 25 V/cm (cm^2/V·min)	μ at 65 V/cm (cm^2/V·min)	τ_{ave} at 25 V/cm (ms)	τ_{ave} at 65 V/cm (ms)
121	0.0018	0.0025	39	0*
383	0.0013	0.0020	100	9
929+1058	0.0005	0.0019	400	12
1857	0.0004	0.0019	525	12

4.3.2 – Pulsed Field Separation Results

Fluorescence intensity profiles for pulsed field separation experiments are shown in Fig. 13. Fluorescence intensity was measured at a distance of 0.5 cm along the nanofilter channel for all experiments. The pulsed field stepped from $\mathbf{E_H}$ = 65 V/cm to $\mathbf{E_L}$ = 25 V/cm. Also, all of peaks 1 through 5 correspond to bands of 121, 383, 929, 1058, and 1857 base pairs of the PBR322 DNA respectively. From the electrophoregrams, it is noticeable that the velocity of all bands decreases as the pulse duration decreases. As the velocity of the molecules reduces, separation resolution also seems to improve. Peak 5,

inseparable from peaks 3 and 4 at long pulse durations, eventually separates from the other peaks once the pulse duration goes below 10 ms.

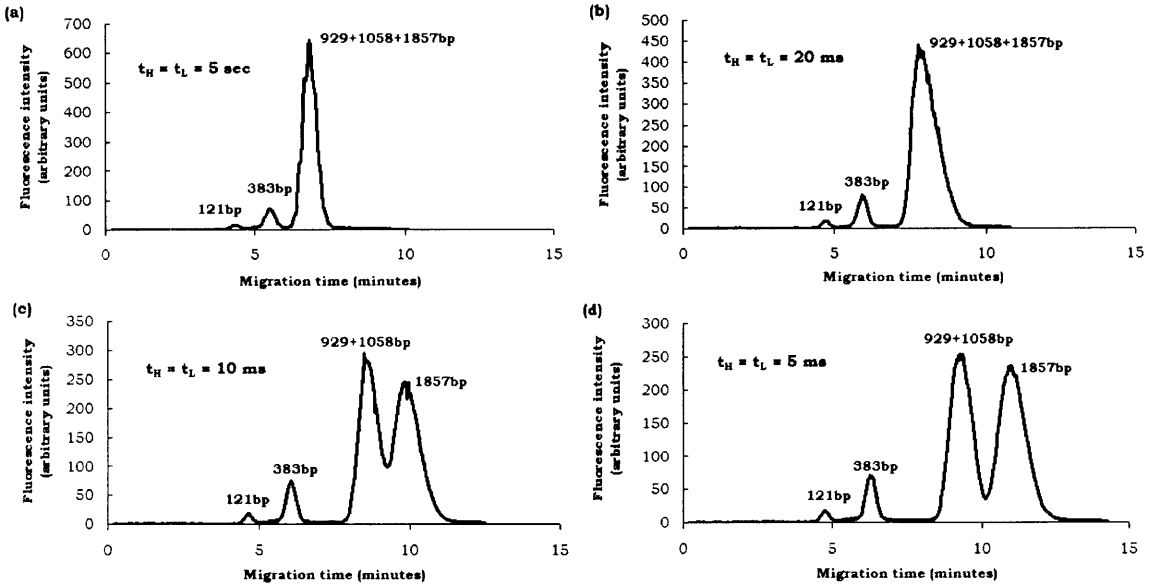

Figure 13. Fluorescence intensity for pulsed field driven experiments.

Table 10. Separation resolution between adjacent peaks of PBR322 DNA for a pulsed field separation experiment.

Bands	R (t_H=t_L=5sec)	R (t_H=t_L=20ms)	R (t_H=t_L=10ms)	R (t_H=t_L=5ms)
121bp & 383bp	1.52	2.05	2.08	2.30
383bp & 929+1058bp	1.20	1.84	2.25	2.54
929+1058bp & 1857bp	0	0	0.63	0.85

5. Discussion

The discussion for separation in the long and short pulse regimes is divided in the first two sections of this chapter. In sections 5.3 and 5.4, two experiments are proposed as the continuation of this work. Finally, an analytical model to predict the behavior of molecules under the short pulse regime is presented in section 5.5.

5.1 – Separation in the Long Pulse Regime

The results for experiments in the long pulse regime were analyzed to compare the experimental velocity values of individual bands with those obtained through equation (2). Tables 11 through 13 show both the experimental and calculated average velocities for separation experiments of Lambda Hind III DNA, SDS proteins, and PBR322 DNA.

Table 11. Comparison between the calculated and experimental average velocities of molecules in Lambda Hind III DNA for long pulse regime fields.

Band	Calculated v_{AV} (cm/min)	Experimental v_{AV} (t_H=t_L=3sec)	Experimental v_{AV} (t_H=t_L=1sec)
23kb	0.097	0.088	0.089
9+6kb	0.082	0.083	0.083
4kb	0.079	0.083	0.083

Table 12. Comparison between the calculated and experimental average velocities of SDS proteins for long pulse regime fields.

Band	Calculated v_{AV} (cm/min)	Experimental v_{AV} (cm/min)
CT-B	0.22	0.22
PHA-L	0.16	0.17
LDL	0.15	0.17

Table 13. Comparison between the calculated and experimental average velocities of molecules in PBR322 DNA for long pulse regime fields.

Band	Calculated v_{AV} (cm/min)	Experimental v_{AV} (cm/min)
121bp	0.10	0.11
383bp	0.08	0.09
929+1058bp	0.07	0.07
1857bp	0.07	0.07

The discrepancies between the calculated and experimental values for the average velocity fall within 13%, and in general there is very good agreement between the two numbers. Although it seems reasonable to estimate the average velocity of molecules under a long pulse field and therefore predict the separation efficiency, it still remains unanswered if better separation could be achieved by utilizing a long pulse field rather than a constant field. Separation resolution of 0.65 was achieved between the 23kb and

9kb bands of Lambda Hind III DNA in the long pulse field regime, compared to a resolution of 2.85 when using a constant field of 40 V/cm. SDS proteins were separated with 0.94 resolution under a constant field of 80 V/cm and with 0.74 resolution for a long pulse field. The long pulse field used for PBR322 DNA experiments did not yield better results than constant field separation either. Separation efficiency under pulsed fields is highly determined by the exact values of the parameters that describe the field. These results are therefore not sufficient to discard the possibility of better separation with fields of long pulses.

Separation resolution between two bands is completely described by the velocities of each band. The difference of the velocities determines how much two bands will separate under a given amount of time, but the values of the velocities themselves determine the amount of time the two molecules will spend traveling down the nanofluidic filter channel. Lower velocities allow for higher spatial separation between the two bands, but at the same time the dispersion of the peaks increases. With higher velocities the spatial resolution decreases, but on the positive side we have that the duration of the experiment also decreases. For simplification, we will restrict the analysis of separation efficiency by measuring the selectivity of separation, that is the velocity difference between the two bands. Fig. 14 illustrates an example of an average velocity versus electric field intensity plot. Parameters v^1_{AV} and v^2_{AV} are the average velocities under a long pulse field of $t_H = t_L$ for bands 1 and 2 respectively, while the variables $v^1(E_H)$, $v^1(E_L)$ and $v^2(E_H)$, $v^2(E_L)$ are the velocities of bands 1 and 2 at the corresponding electric field levels.

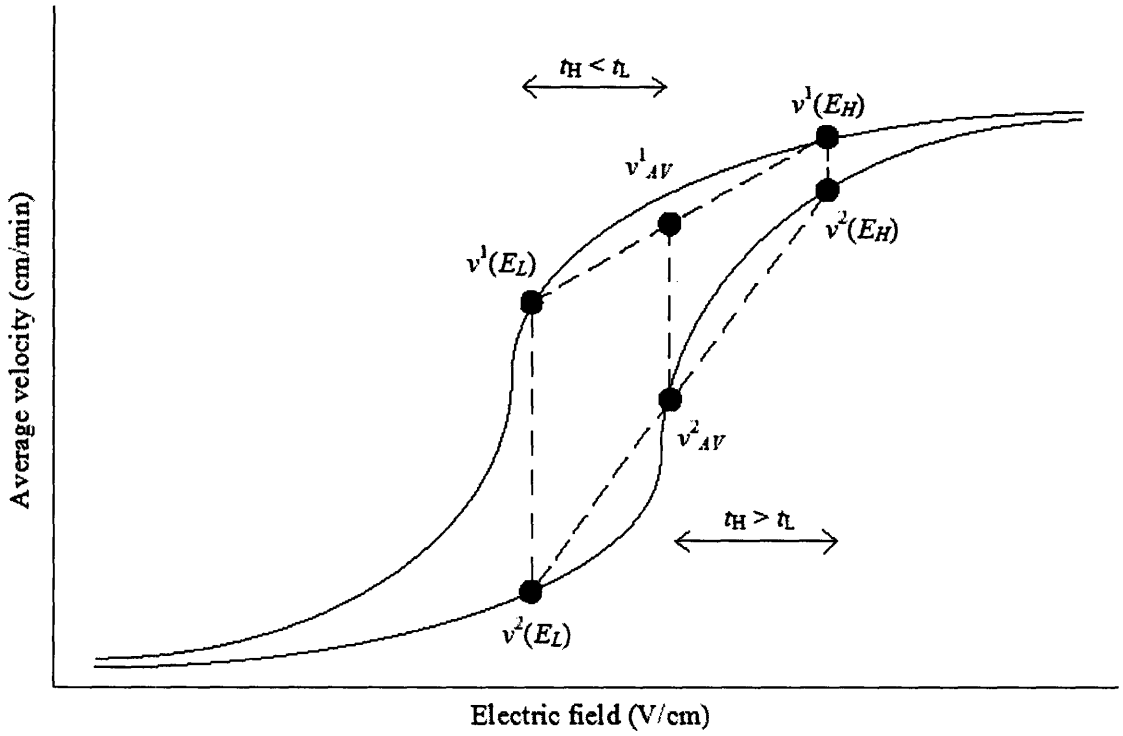

Figure 14. Example of average velocity versus electric field intensity plot.

We want to know if a larger velocity difference is achievable under a long pulse field rather than a constant field. This requirement is described analytically by the inequalities:

$$v^1_{AV} - v^2_{AV} > v^1(E_H) - v^2(E_H) \tag{5}$$

and

$$v^1_{AV} - v^2_{AV} > v^1(E_L) - v^2(E_L), \tag{6}$$

It is assumed that as seen in Fig. 14, that v^1 is larger than v^2 for all electric field values so that the quantity $v^1 - v^2$ is always positive. The difference between the average velocities of two bands in the long pulse regime can be written as:

$$v^1_{AV} - v^2_{AV} = \frac{v^1(E_H) + v^1(E_L)}{2} - \frac{v^2(E_H) + v^2(E_L)}{2}, \tag{7}$$

After adding inequalities (5) and (6), and substituting terms in the right-hand side of the resulting inequality by using (7), the result is that:

$$(v_{AV}^{1} - v_{AV}^{2}) > (v_{AV}^{1} - v_{AV}^{2}), \qquad (8)$$

which is

clearly a contradiction as the terms on both side of the inequality are equal.

This analysis for separation efficiency is valid independently from the shape of the average mobility versus electric field curve. Although the previous analysis is restricted to the case where $t_H = t_L$, it can be shown that the conclusion is true even if the two pulse durations are different. When $t_H > t_L$, the average velocity falls between v_{AV} and $v(E_H)$, and when $t_H < t_L$, it falls between v_{AV} and $v(E_L)$. The velocity difference will always fall between the difference for the constant field cases, and therefore cannot possibly be maximized by applying a long pulse field. The discussion of the application of long pulse fields goes beyond what has been described in this section. A method that involves combining both positive and negative long pulses is proposed in section 5.4 as an alternative to enhance separation efficiency.

5.2 – Separation in the Short Pulse Regime

In the short pulse regime, it is expected for the velocity of molecules to decrease because the pulse duration of the high electric field level $\mathbf{E_H}$ is not large enough to allow every molecule to escape a trap. But, how short does this pulse have to be in order to see a reduction in velocity? If we use the simplest kinetic model (first order kinetics) for the transition between trapped and escaped states, one can conclude that the probability density function $p(t_H)$ that describes the trap escaping process is given by the function:

$$p(t_H) = \frac{1}{\tau_{ave}} e^{-\frac{t_H}{\tau_{ave}}}. \quad (10)$$

The cumulative distribution function $F(t_H)$, which represents the probability that a molecule escapes a trap in a time less than t_H is then described by the equation:

$$F(t_H) = 1 - e^{-\frac{t_H}{\tau_{ave}}}. \quad (11)$$

By analysis of (11) we can tell that for $t_H = 3\tau_{ave}$, the cumulative distribution function $F(t_H) \approx 0.95$, which means that 95% of the molecules will escape one trap during the duration of one pulse. It seems reasonable then to set this value as a threshold, and believe that the velocity of molecules will start to deviate from that in the long pulse regime for values of t_H smaller than $3\tau_{ave}$. At a value of $t_H = 0.7\tau_{ave}$, 50 % of the molecules are expected to escape a trap during the pulse duration.

Fig. 15 shows the plot of average velocity versus pulse duration in the short pulse regime for PBR322 DNA. It is clear from the graph that the average velocity decreases as the pulse duration decreases. The degree until which the velocity is decreased also seems to be larger for the slower molecules. When the pulse duration goes down to 5 ms, the velocity decreases from that in the long pulse regime by a factor of 0.62%, 5.8%, 15.7%, and 28.5% for the 121bp, 383bp, 929+1058bp, and 1857bp bands respectively. The average velocity starts to go down once the pulse duration goes below 20 ms, which is 2.2 times the average trapping time of the 383bp band, and 1.67 times the estimated average trapping time for the 929, 1058, and 1857bp. This result agrees with the idea that the average velocity should start to decrease once the pulse duration is smaller than 3 times the average trapping time. The dashed lines in the graph mark the velocity of the molecules at the average field of 45 V/cm. Interestingly, it seems like the average

velocity converges to the velocity of the molecules at the average field value, which is the result that was reported by Slater et al in [7]. The separation resolution values for the two cases are also extremely similar as shown in Table 14.

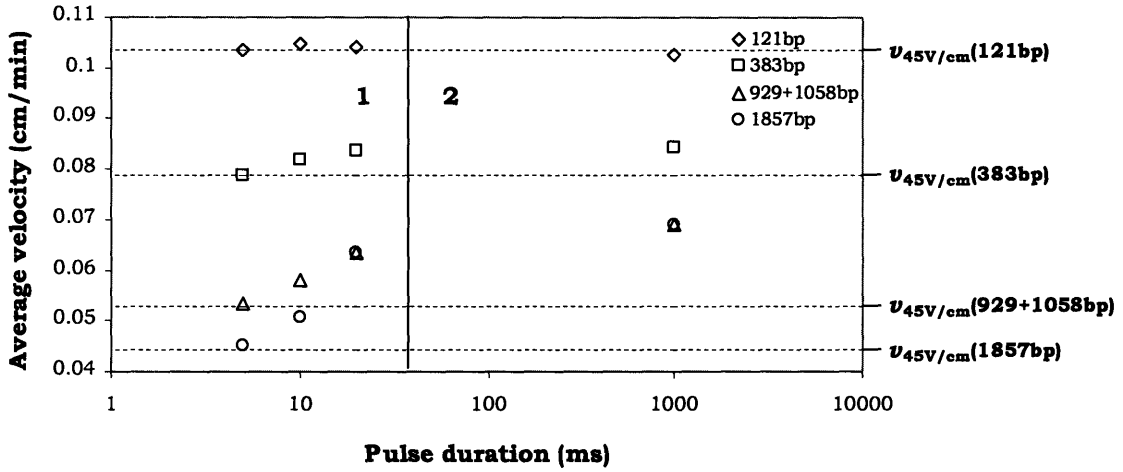

Figure 15. Plot of average velocity versus pulse duration in the short pulse regime field for PBR322 DNA. In region **2** the pulse duration is long enough so that $t_H > 3\tau_{ave}(1857bp)$ and the average velocity is not affected as the pulse duration changes. On the contrary, in region **1** $t_H < 3\tau_{ave}(1857bp)$, so the average velocity decreases as the pulse duration decreases as well. The 1857bp band is used as reference in this case since it has the largest trapping time of all the molecules in the sample and its velocity reduced the fastest in response to a decrease in the pulse duration. The average velocity of each bands converges at the velocity of the average field, which in this case is 45 V/cm.

As the average velocity decreases, the separation resolution between the different bands in the sample increases. As shown in Fig. 13 of section 4.3.2, separation improves to the extent that peaks that were not distinguishable when using a pulse duration of 20ms were almost completely separated when the pulse duration went down to 5ms. Thus separation efficiency can be improved by decreasing the pulse duration of a pulsed field, but does not seem to improve beyond that which is already attainable under constant field situations.

Table 14. Comparison between separation resolution between bands of PBR322 DNA for a constant field of 45 V/cm and a short pulse field of pulse duration equal to 5ms.

Bands	R (45 V/cm)	R (t_H=t_L=5ms)
121bp & 383bp	2.29	2.30
383bp & 929+1058bp	2.52	2.54
929+1058bp & 1857bp	0.82	0.85

The short pulse regime results for SDS proteins are partially similar to those obtained for PBR322 DNA as shown in the plot of Fig. 16. One of the main differences is that the average velocity of the molecules does not seem to converge to the velocity of the molecules at a constant field of 95 V/cm which is the average field. Instead, the average velocity continues to drop to even lower values, which is clearly notable as there are data points that fall below the dashed lines. The second difference is that there seems to be a clear maximum in the average velocity when the pulse duration is 50ms. The

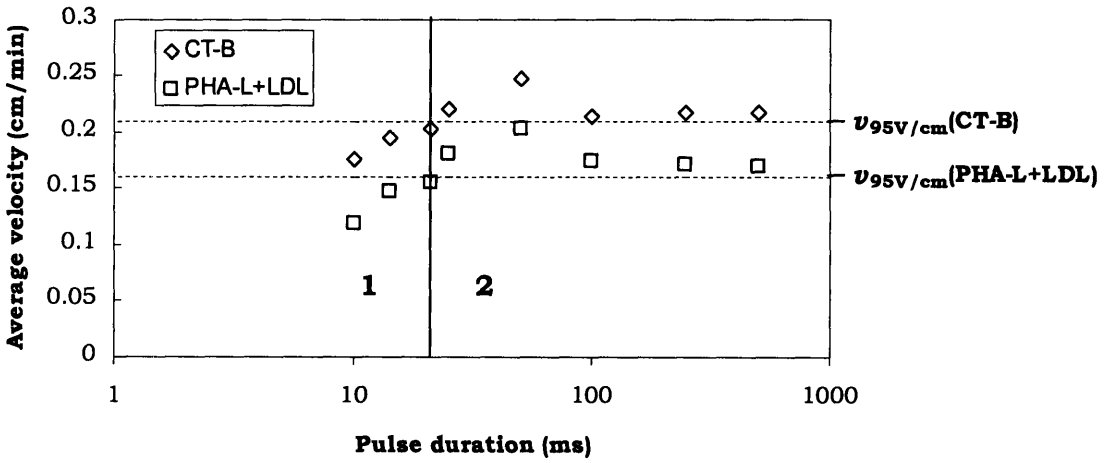

Figure 16. Plot of average velocity versus pulse duration in the short pulse regime field for SDS proteins. In region **2** the pulse duration is long enough so that $t_H > 3\tau_{ave}$(PHA-L+LDL) and the average velocity is not affected as the pulse duration changes. On the contrary, in region **1** $t_H < 3\tau_{ave}$(PHA-L+LDL), so the average velocity decreases as the pulse duration decreases as well. The PHA-L+LDL band is used as reference in this case since it has the largest trapping time of all the molecules in the sample and its velocity reduced the fastest in response to a decrease in the pulse duration. The average velocity of each bands converges at the velocity of the average field, which in this case is 95 V/cm.

possibility of a maximum at some intermediate pulse duration in the short pulse regime is not discarded. Slater et al proposed that a maximum velocity was attainable when t_H = $1.25\tau_{ave}$. The average trapping time mentioned is that for higher field in the pulsed field, which in this case is 7ms. The resonant pulse duration would then be $t_H \approx$ 9ms, which is far away from the presumed resonant pulse duration of 50ms.

The average of velocity of the CT-B molecules decreases by 18.9% as the pulse duration is reduced from 500ms down to 10ms, while that of the PHA-L and LDL molecules decreases by 30.6% for the same pulse duration interval.

5.3 – Proposed Experiment #1: Band Selective Elution

As discussed in the previous section, the pulse duration at which the velocity a molecule starts decrease should be very near three times the average trapping time at the high field level of the pulsed field. In the experiments that have already been performed, the difference between the average trapping times of two bands in a sample is very small. For example, the difference between the average trapping times of 383bp and 929bp bands of PBR322 DNA was estimated to be only 3ms. The value of E_H for those pulsed field experiments was 65 V/cm. At 25 V/cm the average trapping times for the 383bp and 929bp bands are much larger, 100ms and 400ms respectively. The difference between the two times is also considerably large at 300ms.

If for example the E_H was set to be 25 V/cm, the results of a short pulse regime separation experiment could be very different. Consider that t_H was then set to be 300ms so that $t_H = 3\tau_{ave}$ for the 383bp band, and $t_H = 0.75\tau_{ave}$ for the 929bp band. 95% of the 383bp molecules would be able to escape a trap during the pulse duration, while only 50% of the 929bp molecules are to escape. Having a large difference between the average

trapping times of two bands allows setting the pulse duration at an intermediate point in which migration of one band is stimulated while migration of a second band is considerably retarded. This method involves using low electric field levels so the duration of a separation trial could be longer than normal. On the other hand, the method allows to user to choose the point at which the sample will be fractionated, and by repeatedly running this process it is possible to completely separate all the bands contained in a sample.

5.4 – Proposed Experiment #2: Bidirectional Transport

The non-linearity of the mobility versus electric field profile together with application of pulsed electric fields presents itself as an opportunity for new separation methods that could potentially increase the efficiency of current methods while facilitating the ease of the process. A possible separation method that achieves bidirectional transport of two groups of molecules is described in this section. The applied pulsed field is identical to the one used in previous experiments, with the exception that the field level $\mathbf{E_L}$ is now negative. The purpose is to achieve migration of two bands or group of molecules in opposite directions, so that $v^1_{AV} < 0$, and $v^2_{AV} > 0$. After altering equation (1) so that it takes into consideration the fact that the velocity at field $\mathbf{E_L}$ is negative, these inequalities can be rewritten as:

$$\frac{v^1(E_H) - v^1(E_L)\frac{t_L}{t_H}}{1+\frac{t_L}{t_H}} < 0 \qquad (12)$$

and

$$\frac{v^2(E_H)-v^2(E_L)\frac{t_L}{t_H}}{1+\frac{t_L}{t_H}}>0, \tag{13}$$

where all variables and parameters are as described in previous sections. The denominators of the left-hand sides of (10) and (11) cannot attain negative values so that the inequalities are simplified to:

$$v^1(E_H)-v^1(E_L)\frac{t_L}{t_H}<0 \tag{14}$$

and

$$v^2(E_H)-v^2(E_L)\frac{t_L}{t_H}>0. \tag{15}$$

After arranging terms and combining both inequalities we are left with:

$$\frac{v^1(E_H)}{v^1(E_L)}<\frac{t_L}{t_H}<\frac{v^2(E_H)}{v^2(E_L)}, \tag{16}$$

therefore defining a specific range of pulse duration ratios for which bidirectional transport is possible. The method was simulated using the data obtained for pulsed field separation of PBR322 DNA. Fig. 17 shows the plot of average velocity versus pulse duration ratio for a pulse field with $\mathbf{E_H}$ = 65 V/cm and $\mathbf{E_L}$ = -25 V/cm. Bidirectional transport is obtained when the pulse duration ratio is held between 4.25 and 9.9.

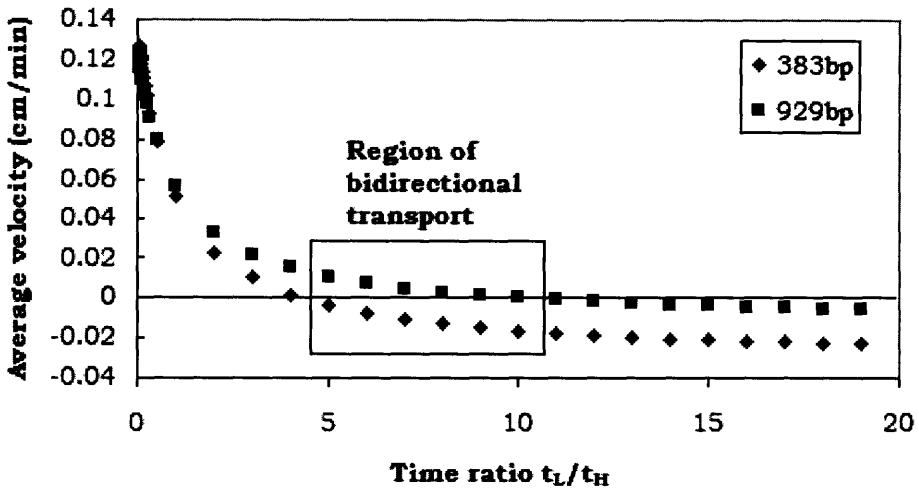

Figure 17. Average velocity versus pulse duration ratio for two bands in PBR322 DNA.

In-depth analysis of the problem at hand shows that bidirectional transport happens after the order of elution of the two bands is switched. Fig. 18 zooms into the range of pulse duration ratios below unity. For very small duration ratios the average velocity approaches that of the molecules under a constant field of $\mathbf{E_H}$ = 65 V/cm. When the pulse duration ratio is approximately 0.5 the average velocity of the 383bp molecules goes below that of the 929bp molecules. The velocity of the 383bp band continues to decrease more rapidly, eventually crossing the zero velocity line while the velocity of the 929bp is still positive.

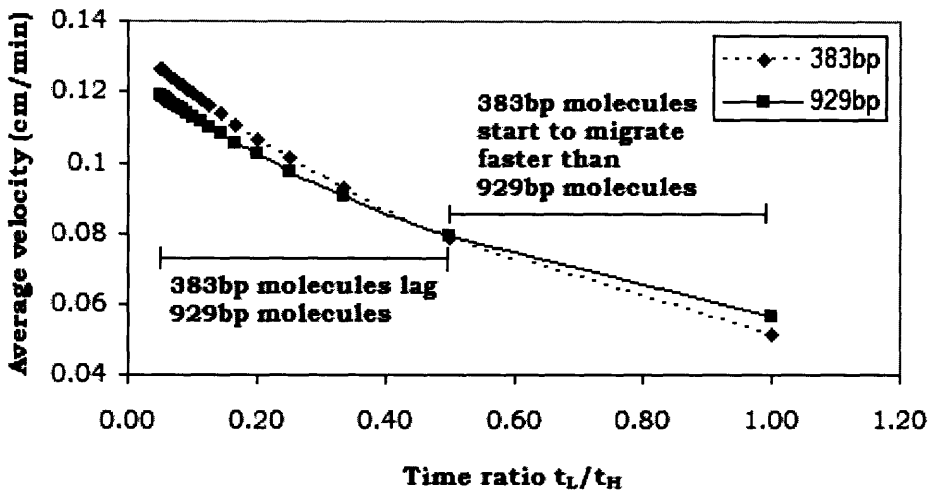

Figure 18. Average velocity versus pulse duration ratio for two bands in PBR322 DNA.

Bidirectional transport has some advantages over traditional size fractionation in a nanofluidic filter channel. Consider the device of simplified geometry presented in Fig. 19. The biomolecule sample is driven through the loading reservoir to the middle of the length of the nanofluidic filter channel. A pulsed field is then applied across the sample collection reservoirs as to induce bidirectional transport of two groups of molecules. Driving the separated bands into different reservoirs allows for simpler collection of the samples. The second advantage that comes along with separation by bidirectional transport is that the exact point of fractionation can be controlled by selecting the appropriate electric field and pulse duration values for the pulsed field.

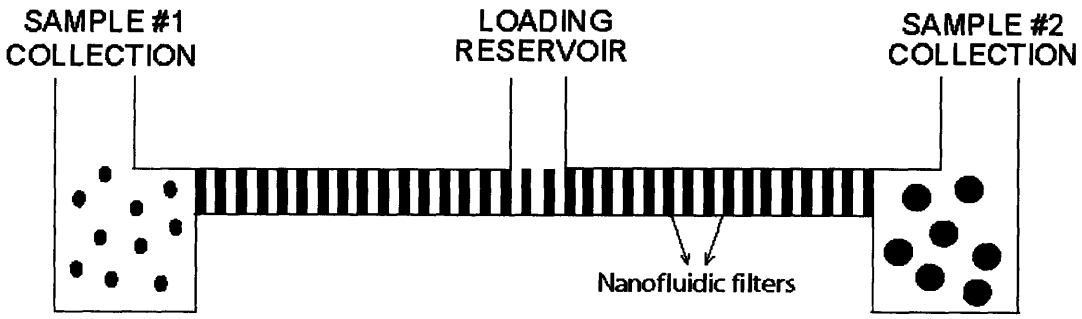

Figure 19. Geometry of proposed channel for bidirectional transport.

5.5 – Analytical Model for the Short Pulse Regime: The Binomial Distribution

Analysis of separation in the short pulse regime is not straightforward and requires probabilistic methods to define the distribution of molecules along the length of the nanofluidic channel for a given pulse duration. The following model describes the distribution of molecules after some time t given certain assumptions. The first assumption is that the length of the low electric field level t_L is high enough so as to carry molecules that have escaped a trap onto the face of the next thin region, but not as long so as to make the molecules escape a second trap. The second assumption is that a molecule only escapes one trap per period of the pulsed field ($t_H + t_L$). If the length of the high electric field level t_H, is less than three times the average trapping time, the model starts to fail as the average velocity decreases misleadingly. Because a molecule is not allowed to escape more than one trap per period, the model takes it as if it remained floating around until the end of the pulse duration t_H.

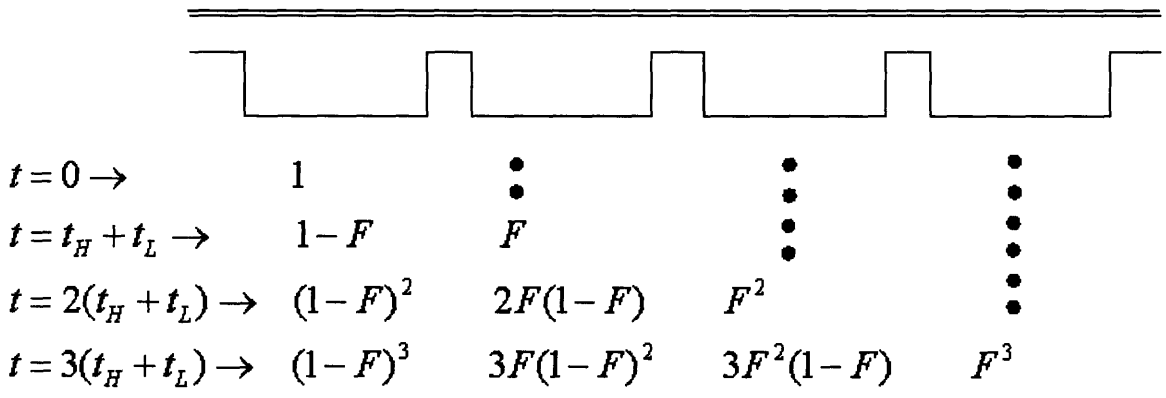

Figure 20. Distribution of molecules after a short pulse field has been maintained for a length of time t. At $t = 0$ all molecules reside in the first deep region of the channel. After one pulse of duration t_H, a fraction F(t_H) manage to escape the first trap, while the rest still lags behind. Continuous characterization of this process shows that the distribution of molecules along the length of the channel is binomial and depends on the number of periods, $t_H + t_L$, that have occurred within the time t.

Fig. 20 shows how the distribution of molecules across the length of the nanofluidic filter yields to be a binomial distribution that depends on the period of the applied pulsed field. The number of periods N that have occurred within a time t is given by:

$$N = \frac{t}{t_H + t_L}. \tag{17}$$

The probability p_S that a molecules will reside in the n^{th} deep region of the channel after a time t is then given by the binomial distribution equation:

$$p_S(n \mid N) = \frac{N!}{n!(N-n)!} F^n (1-F)^{N-n} \quad . \tag{18}$$

Simply enough, for a binomial distribution that means that the average molecule will reside in deep region n_{AV} given by:

$$n_{AV} = N \times F$$

The approximate position in the channel and the average velocity of the molecule are then given by the equations:

$$d_{AV} = N \times F \times L, \tag{19}$$

and

$$v_{AV} = \frac{d_{AV}}{t} = \frac{N \times F \times L}{t} = \frac{F \times L}{t_H + t_L}. \tag{20}$$

The model delivers a first order approximation of the average velocity of a molecule under a short pulse field, and seems to connect with the average velocity expected in the long regime. Fig. 21 shows the results of simulation ran using the binomial distribution model. The simulation considers a sample of PBR322 DNA being separated with a pulsed field that alternates between E_H = 65 V/cm and E_L = 25 V/cm. In

order to comply with the assumptions of the model, t_L was set to t_{travel} = 100ms. We know that as the pulse duration t_H goes to zero, the average velocity goes to that obtained at the low field level E_L = 25 V/cm. The average velocity was then plotted only until it reached the velocity obtained for a constant field of 25 V/cm. The plot is separated into 4 different regions, because the average velocity of some molecules may not be valid in a certain region. More precisely, we believe that approximately when the pulse duration exceeds three times the average trapping time of a molecule, the model is no longer valid for that molecule. That is because one of the assumptions of the model is violated, t_H is already long enough so as to escape more than one trap within one period of the pulsed field, but the model does not allow for that to happen. Therefore, the average velocity

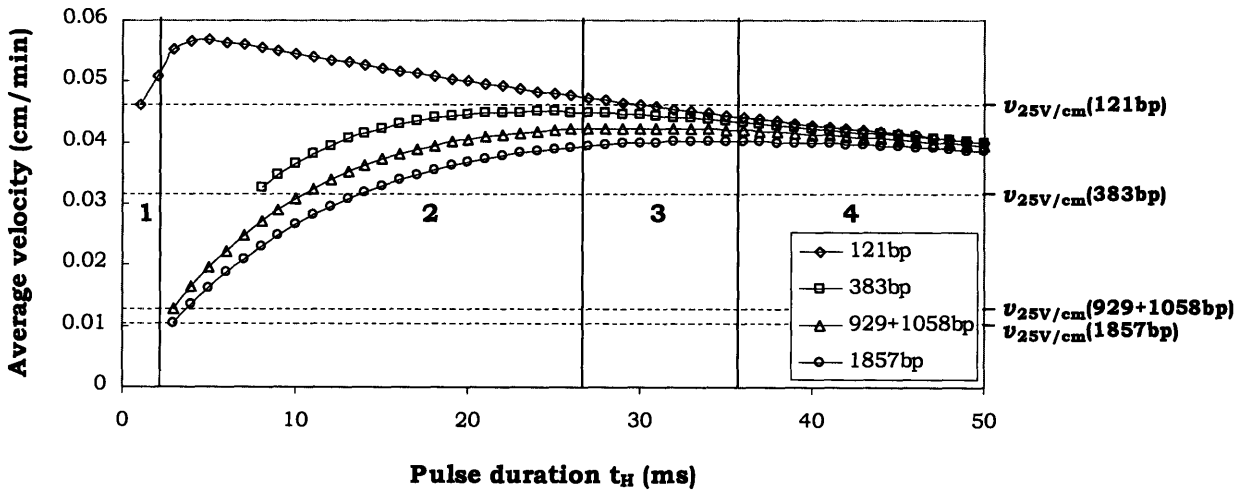

Figure 21. Simulated plot of average velocity versus pulse duration with the binomial distribution model. The simulation considers a pulsed field that alternates between E_H = 65 V/cm and E_L = 25 V/cm, with low field pulse duration t_L = 100ms. In Region **1**: $3\tau_{ave}(121bp) < t_H < 3\tau_{ave}(383bp)$, Region **2**: $3\tau_{ave}(383bp) < t_H < 3\tau_{ave}(929+1058bp)$, Region **3**: $3\tau_{ave}(929+1058bp) < t_H < 3\tau_{ave}(1857bp)$, and in Region **4**: $3\tau_{ave}(1857bp) < t_H$. Approximately when the pulse duration exceed three times the average trapping time of a molecule, the model is no longer valid for that molecule. For example, Region **2** is clearly not valid for the 121bp band since the average velocity decreases with an increase in pulse duration and we know that experimentally this is not true.

starts to decrease as the pulse duration increases, which is not the result obtained experimentally. Following this argument, the results in Region **4** are not valid for any of the bands of PBR322 DNA. Only the largest band, 1857bp, is valid in Region **3**. In this region the band is already approaching the long pulse regime. The average velocity in Region **3** obtained from the binomial distribution model for the 1857bp band is ~0.040 cm/min, while that obtained through equation (1) is ~0.037 cm/min, a deviation of only 7%. Although agreements with the results in the short pulse regime would have to be tested experimentally, the data shows the right trends as the average velocity falls down in a similar manner as it does in the experiments performed for PBR322 DNA.

6. Conclusion

Implementation of pulsed electric fields to the separation of biomolecules in nanofluidic filter channels has proven challenging and exciting. Separation under long pulse regime promises little except for the intriguing possibility of being able to induce bidirectional transport. This method could definitely prove important for sample collection in one-dimensional devices, which is currently one of the main difficulties confronted with these types of devices. The results obtained for separation under the short pulse regime are far more interesting. Gladly, the experimental results fairly agreed with the Monte Carlo simulations performed by Slater et al [7,11]. It was observed that for small pulse durations, the average velocity of molecules decreased as the pulse duration also decreased. This occurs because the escaping dynamics of a molecule are affected when the pulse duration comes close to the average trapping time of the molecule. By reducing the pulse duration, the probability of escape also decreases. Smaller molecules are affected more extensively by the reduction in pulse duration, and that accounts for the

increase in the velocity difference between bands of the sample as the pulse duration is decreased. By choosing an intermediate pulse duration, larger than the average trapping time of one group of molecules but smaller than the average trapping time of another group of molecules, it might be possible to achieve ever greater separation selectivity. Achieving major analytical understanding of separation under the short pulse regime might require the use of computer simulations, as only first-order approximations can be made without further processing power.

Acknowledgements

I would like to thank my thesis supervisor, Prof. Jongyoon Han, for dedicating his time unconditionally to making the success of this project possible. I would also like to give special thanks to Jianping Fu, for his assistance as an experienced researcher, and for fabricating the nanofluidic filter devices used in this project. I greatly appreciate the help and guidance provide by my fellow lab members: Dr. Yong-Ak Song, Pan Mao, Hansen Bow, and Ying-Chih Wang.

The devices were fabricated at the Microsystems Technology Laboratories (MTL) at MIT. Funds for this project provided by: NSF CTS-0347348, Singapore-MIT Alliance, and CE programme FRP-1.

References

[1] P.-A. Auroux, D. Iossifidis, D. R. Reyes, and A. Manz, "Micro Total Analysis Systems. 2. Analytical Standard Operations and Applications," *Analytical Chemistry*, vol. 74, pp. 2637-2652, 2002.

[2] D. R. Reyes, D. Iossifidis, P.-A. Auroux, and A. Manz, "Micro Total Analysis Systems. 1. Introduction, Theory, and Technology," *Analytical Chemistry*, vol. 74, pp. 2623-2636, 2002.

[3] J. Han, and H. G. Craighead. "Entropic trapping and sieving of long DNA molecules in a nanofluidic channel," Journal of Vacuum Science & Technology, A: Vacuum, Surfaces, and Films, 17, 2142 (1999).

[4] J. Fu, P. Mao, J. Han. "Moelcular Sieving in periodic free-energy landscapes created by an array of nanofluidic filters". Applied Physics Letters, 87, 263902(2005).

[5] D.C. Schwartz, C.R. Cantor. Cell, 37, 67-75 (1984).

[6] J. Sudor, M. Novotny. "Separation of Large DNA Fragments by Capillary Electrophoresis under Pulsed-Field Conditions". Analytical Chemistry, 66, 2246-2450 (1994).

[7] F. Tessier and G.W. Slater. "Strategies for the separation of polyelectrolytes based on non-linear dynamics and entropic ratchets in a simple microfluidic device". Applied Physics A 75, 285-291 (2002).

[8] G.W. Slater, H. Guo, G. Nixon. "Bidirectional Transport of Polyelectrolytes Using Self-Modulating Entropic Ratchets". Physical Review Letters, 78, 1170-1173 (1997).

[9] J. Sudor and M. V. Novotny. "Separation of Large DNA Fragments by Capillary Electrophoresis Under Pulsed-Field Conditions". Analytical Chemistry, 66, 2446 (1994).

[10] J. Han, and H. G. Craighead. "Characterization and Optimization of an Entropic Trap for DNA Separation," Analytical Chemistry, 74, 394-401 (2002).

[11] F. Tessier, G.W. Slater. "Separation of Long Polyelectrolytes in a Microfluidic Channel with Constrictions: A Monte Carlo Study".

[12] G. Nixon, G.W. Slater. "Entropic trapping and electrophoretic drift of a polyelectrolyte down a channel with a periodically oscillating width". Physical Review E, 53, 4969-4980 (1996).

[13] J. Han, S.W. Turner, and H.G. Craighead. "Entropic Trapping and Escape on Long DNA Molecules at Submicron Size Constriction". Physical Review Letters, 83, 1688-1691 (1999).